THERMAL ANALYSIS, EPR AND XPS STUDY OF VANADYL(IV) OXALATE BEHAVIOR ON THE CERIA SURFACE

J. Matta, D. Courcot, E. Abi-Aad and A. Aboukaïs[*]

Laboratoire de Catalyse et Environnement – E.A.2598, Université du Littoral – Côte d'Opale, MREID, 145, avenue Maurice Schumann, F-59140 Dunkerque, France

Abstract

The thermal decomposition of vanadyl oxalate supported on CeO_2 solid in a flow of dried air was analysed by thermogravimetry (TG) and differential scanning calorimetry (DSC) from room temperature up to 350°C. TG and DSC results have demonstrated that after the impregnation of CeO_2 solid by a vanadyl oxalate solution, cerium and vanadium(V) oxalates were evidenced. This latter compound seems attached to cerium(III) of the partial reduced CeO_2 phase. This result was confirmed with the electron paramagnetic resonance (EPR) and X-ray photoelectron spectroscopy (XPS) techniques.

Keywords: cerium oxalates, EPR, thermal analysis, vanadium oxalates, XPS

Introduction

One of the most important applications of CeO_2 is in the formulation of modern three-way catalysts (TWC) used in automotive exhaust gas cleaning systems [1–4]. It is well known that CeO_2 is able to act as an efficient oxygen buffer by releasing/storing O_2 due to its capability to undergo effective reduction and reoxidation under rich and lean conditions respectively [4–6]. Thus, the decrease of sensitivity of Ce-containing TWC to oscillations of a gas mixture composition and, consequently, enhancement of their red-ox properties occur due to compensation of a gas composition fluctuations by high mobility of lattice oxygen in CeO_2.

In parallel, vanadia supported on various oxide carriers is widely used as a catalyst in different oxidation processes [7–8]. It is also proved to be quite effective for the selective catalytic reduction (SCR) of nitric oxide NO [9]. It has been demonstrated that the selectivity and activity of these catalysts depend on, among other factors, the vanadium loading, calcination temperature, type of support and its surface acidity [10].

———————
* Author for correspondence: E-mail: aboukais@univ-littoral.fr

In general, the catalytic activity of mixed oxide systems depends on many factors particularly the method of preparation and the nature of precursors. Recently [11–17], considerable attention has been devoted to the oxalate ligand as a structural unit in the preparation of mixed oxides. Since the oxalate group can function as a bisbidentate ligand, coordination to two metal ions affords a wide variety of polynuclear complexes.

The principal objective of the present work is to identify the intermediate complexes formed during the preparation of the vanadium-cerium oxide catalysts from the ceria phase and vanadyl-oxalate taken as a precursor.

Experimental

Ceria (CeO_2) was prepared by precipitation of cerium hydroxide from $Ce(NO_3)_3 \cdot 6H_2O$ with a NaOH solution as described elsewhere [18]. The solid was calcined at 500°C for four h under a flow of dried air. Subsequently, to perform a classical impregnation method, a solution of vanadyl oxalate VOC_2O_4 was added on ceria to prepare xV10Ce samples with different V/Ce atomic ratios (x=1.08, 1.67, 2.73 and 5.06). After filtration, these freshly prepared solids were dried at 100°C and after were analyzed with the X-ray diffraction technique. Only the XRD lines corresponding to the CeO_2 phase were observed. No trace of any other crystallized phase was obtained on all the samples.

Thermal analysis measurements were performed using a Netzsch STA 409 apparatus equipped with a microbalance. Simultaneous thermogravimetric and differential scanning calorimetric (TG-DSC) curves were obtained while the dried xV10Ce samples were heated from room temperature to 350°C with a rate of 5°C min^{-1} under a flow of air (75 mL min^{-1}).

Electron paramagnetic resonance (EPR) measurements were performed at –196°C on an EMX Bruker spectrometer. A cavity operating with a frequency of ~9.5 GHz (X-band) was used. The magnetic field was modulated at 100 kHz. The g values were determined from precise frequency and magnetic field values.

XPS spectra are acquired with a Leybold-Heraeus LHS 10 spectrometer with an AlK$_\alpha$ anticathode ($h\nu$=1486.6 eV). The samples are crushed into a fine powder and pressed on an indium support. The spectra are recorded under high vacuum (10^{-8} torr). The binding energies are determined by using the C1s peak at 284.7 eV for standardisation.

Results and discussion

Thermal analysis study

Figure 1 illustrates TG and DSC curves of the freshly prepared xV10Ce samples. DSC curves reveal an endothermic dehydration peak between 50 and 170°C. This dehydration process was followed by two or three exothermic peaks. The DSC and TG data indicate that the exothermic event was closely related to the presence of vana-
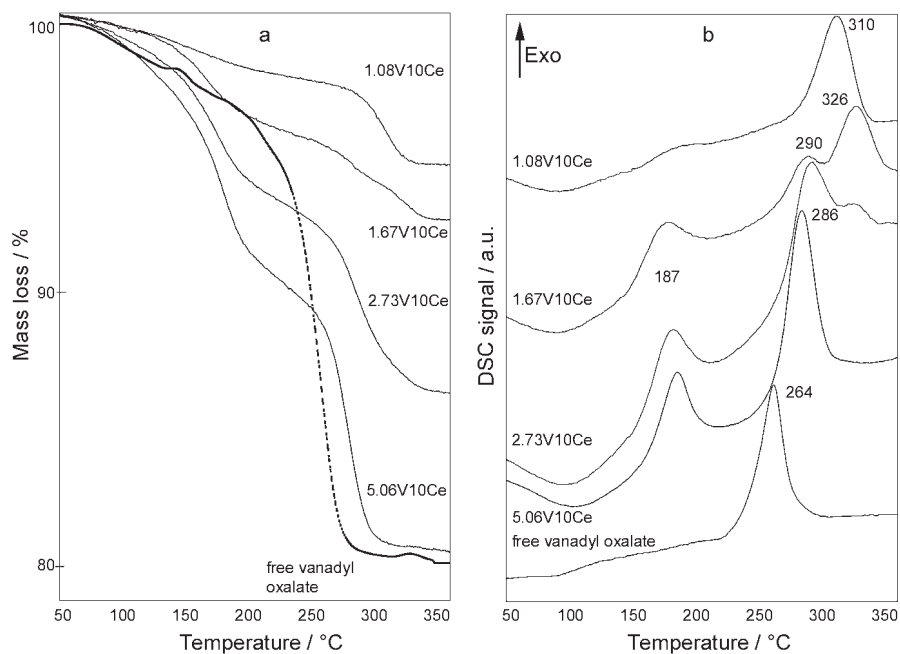
Fig. 1 TG (a) and DSC (b) curves obtained on 1.08V10Ce, 1.67V10Ce, 2.73V10Ce, 5.06V10Ce and free vanadyl oxalate samples after heating the solids under a flow of dried air from room temperature to 350°C

dium in the samples. In fact, for the 1.08V10Ce sample, only two exothermic peaks at 187 and 310°C were observed. The intensity of the first one increased with the vanadium concentration whereas that of the second peak decreased and shifted towards high temperatures (326°C) and finally disappeared for the 5.06V10Ce sample. In parallel, an exothermic peak in the temperature range of 285–295°C appeared and its intensity increased with vanadium content.
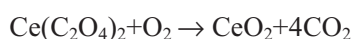
Exothermic peak at 310°C

In order to evidence the origin of this peak, CeO_2 phase, already calcined at 500°C, was impregnated by oxalic acid instead of vanadyl oxalate. After heating this freshly prepared solid up to 350°C, two endothermic peaks at 188 and 223°C and another exothermic at 310°C were observed (Fig. 2). The temperature of the exothermic peak is the same as that obtained for the 1.08V10Ce sample (310°C). This can unambiguously indicate that the above peak is due to the decomposition of cerium oxalate. Similar results have been already obtained in literature [19–21]. This latter product can be formed by a simple reaction between oxalic acid and CeO_2 surface:

$$CeO_2 + 2H_2C_2O_4 \rightarrow Ce(C_2O_4)_2 + 2H_2O$$
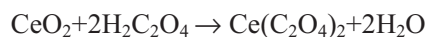
or by simple exchange between the vanadyl group and cerium when vanadyl oxalate solution is added to ceria:

$$CeO_2 + 2VOC_2O_4 \rightarrow Ce(C_2O_4)_2 + 2VO^{2+} + 2O^{2-}$$

In order to confirm this attribution, a free oxalic acid was heated separately, in absence of the CeO_2 phase. Two endothermic peaks at 189 and 218°C were obtained (Fig. 2) and no exothermic peak was detected. The absence of the exothermic peak at 310°C confirms our supposition that the similar peak obtained at the same temperature in the case of the 1.08V10Ce sample was due to the decomposition of cerium oxalate according to the following reaction [19]:

$$Ce(C_2O_4)_2 + O_2 \rightarrow CeO_2 + 4CO_2$$

When the vanadyl oxalate concentration increased on the CeO_2 surface, the exothermic peak shifted towards high temperatures but its intensity decreased. This shift can be interpreted by the formation on the ceria surface of free vanadyl oxalate in the form of agglomerates. Such form of oxalates are inert with respect to the ceria surface and block the formation of cerium oxalate responsible of the exothermic peak presence.
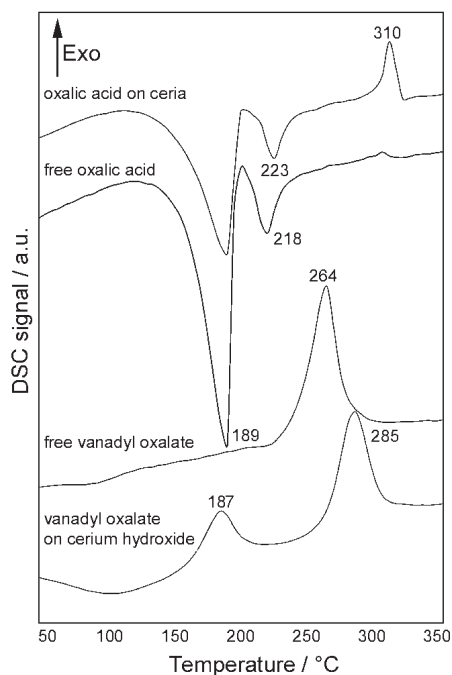
Fig. 2 DSC curves obtained on oxalic acid/CeO_2; free oxalic acid; free vanadyl oxalate and vanadyl oxalate/cerium hydroxides samples after heating the solids under a flow of dried air from room temperature to 350°C

Exothermic peak at 286–290°C

The intensity diminution of the exothermic peak at 310°C with the vanadium concentration and the appearance of a new exothermic peak in the range of 286–290°C were related to the presence of an excess of vanadyl oxalate. Indeed, when this latter complex was heated in the absence of ceria up to 350, a single exothermic peak at 264°C was obtained. From the mass loss measurement after this treatment, the peak was attributed to the decomposition of vanadyl oxalate:

$$2VOC_2O_4 + 3/2O_2 \rightarrow V_2O_5 + 4CO_2$$

The exothermic peaks obtained in the temperature range of 286–290°C on the xV10Ce samples can also be due to the decomposition of the vanadyl oxalate interacting with ceria surface:

$$2VOC_2O_4/CeO_2 + 3/2O_2 \rightarrow V_2O_5/CeO_2 + 4CO_2$$

Indeed, on one side, the intensity of this peak increased with the vanadium concentration and on the other side the decomposition temperature decreased while the vanadium contents increased and tended towards that corresponding to the decomposition of the free vanadyl oxalate (Fig. 2).

Exothermic peak at 187°C

The exothermic peak obtained at 187°C was assigned to the thermal decomposition of vanadium(V) oxalate adsorbed on the ceria surface. Indeed, during the impregnation of the ceria phase by the vanadyl oxalate solution, a brown color on the CeO_2 surface was remarked in the beginning of the preparation. This color changed from brown to brown-dark when the concentration of vanadyl on CeO_2 increased. In parallel, the intensity of the exothermic peak increased. This peak was not obtained when an oxalic acid solution was added separately on CeO_2 and V_2O_5 phases. This confirms that its appearance is not due neither to cerium oxalate nor to vanadium(V) oxalate but it seems to be due to a complex of cerium-vanadium(V) oxalate. In addition, in order to confirm the attachment of the vanadium(V) oxalate to the cerium in ceria, the vanadyl oxalate solution was added on a mixture of cerium hydroxides $Ce(OH)_3$ and $Ce(OH)_4$ phases (Fig. 2). An intense exothermic peak at 187°C was obtained by heating the freshly impregnated solid. This peak intensity was larger than those obtained in the case of the CeO_2 phase. The increase in the intensity can be related to the presence of Ce^{3+} with Ce^{4+} ions in the hydroxides. From this result, it seems that the complex corresponding to the exothermic peak at 187°C is formed by vanadium(V) oxalate attached to cerium(III). In order to demonstrate how this complex can be obtained from vanadyl-oxalate and CeO_2, EPR and XPS study was performed on the xV10Ce samples.

EPR study

Figure 3 shows EPR spectra obtained on the untreated xV10Ce samples. For 1.08V10Ce sample, two superimposed signals denoted by A and B with $g<2$ were observed on the solids. Another signal formed of a well-resolved hyperfine structure of six lines characteristic of Mn^{2+} ions present in the solid as impurities. A and B signals characterized by $g_{\perp(A+B)}$=1.967; $g_{//(A)}$=1.940 and $g_{//(B)}$=1.947 were attributed to the presence of two different Ce^{3+} [f^1 ions; $g_e>g_\perp>g_{//}$] sites in the solid. Similar signals were observed in literature [18, 22] and assigned to Ce^{3+} ions or more precisely to an interaction between conduction electrons and 4f orbital of Ce^{4+} ions in the CeO_2 matrix. These signals were also present on the EPR spectrum of the ceria support before impregnation. No trace of an EPR signal indicating the presence of a vanadyl group in the 1.08V10Ce sample since the vanadium(IV) in such a group is paramagnetic possessing a single electron in the 3d orbital. This indicates that this paramagnetic species was oxidised into vanadium(V) which is diamagnetic and undetectable in EPR. On the contrary, for xV10Ce samples where x=1.67, 2.73 or 5.06, a symmetric signal centered at g=1.96 with a peak-to-peak width changing with the vanadium content was detected. Similar signals were obtained in different matrices [23–25] and were attributed to vanadium(IV) of vanadyl groups.The presence of the vanadyl EPR signal on the samples is due to the excess vanadyl-oxalate remaining on CeO_2 phase after a part has reacted with this latter phase to transform the vanadium(IV) into vanadium(V). Indeed, the intensity of this signal increased with the vanadyl-oxalate concentration whereas the peak-to-peak width decreased from 320 to 256 G when the sample was changed from 1.67V10Ce to 5.06V10Ce. The decrease in
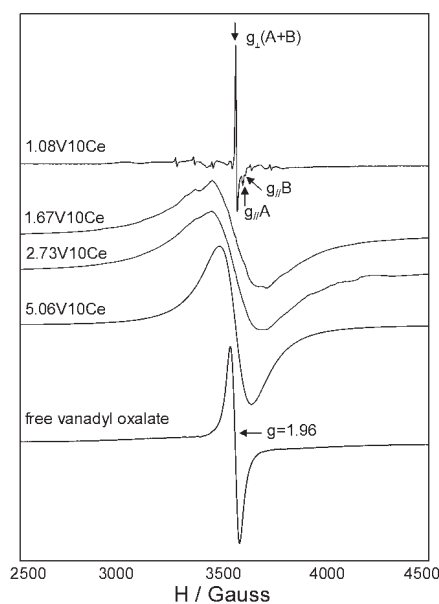
Fig. 3 EPR spectra obtained on free vanadyl oxalate, 1.08V10Ce, 1.67V10Ce, 2.73V10Ce and 5.06V10Ce samples

the width of the signal with increasing the concentration of vanadyl is caused by strong spin-spin exchange in these vanadyl paramagnetic species [26]. For this reason, the EPR signal obtained for the free vanadyl oxalate having a peak-to-peak width (48 G) smaller than those measured for xV10Ce samples (Fig. 3). The relative intensities of signals were calculated by double integration. Table 1 illustrates the percentage in mass of the vanadyl oxalate present in each sample and the percentage of vanadium(IV) species detected by EPR and consequently the percentage of vanadium(IV) oxidised into vanadium(V). This latter percentage was calculated by a simple difference between the two first percentages. These results indicate that by increasing the vanadyl oxalate concentration on the ceria surface, the formation of vanadium(V) became more important. This evolution is compatible with that obtained for the exothermic peak at 187°C.

Table 1 Different percentages of V(IV) species deduced from EPR spectra of xV10Ce samples

| Sample	VOC_2O_4/%	Relative intensity/a.u.	V(IV) detected/%	V(IV)$\rightarrow$V(V)/%
VOC_2O_4	100.00	728.0	100.00	–
1.08V10Ce	8.84	–	–	8.84
1.67V10Ce	13.07	9.2	1.21	11.86
2.73V10Ce	19.73	20.3	2.79	16.94
5.06V10Ce	31.30	37.5	5.15	26.15

XPS study

Figure 4 illustrates $V2p_{3/2}$, Ce3d, O1s and C1s XPS spectra relative to 1.67V10Ce and 5.06V10Ce samples.

$V2p_{3/2}$ component peaked at 517.1 eV (1.67V10Ce) is in agreement with the values obtained for vanadium(V) species in different matrices [27, 28]. When the vanadium concentration increased (5.06V10Ce), a new XPS peak at 516.2 eV appeared (Fig. 4a). This peak was attributed to vanadium(IV) of vanadyl oxalate [29–31]. This result confirms our attribution of the exothermic peak (286–290°C) in the thermal analysis part to vanadyl oxalate.

Figure 4b illustrates Ce3d XPS spectra relative to 1.67V10Ce and 5.06V10Ce samples. Apparently, the six components observed on the spectra could be assigned unambiguously to Ce^{4+} species by comparison with data reported in literature [18, 32–34]. Compared to XPS spectrum of pure CeO_2, our spectra are not well-resolved. From the feature of these spectra, the superposition of Ce^{3+} XPS lines is predicted. In fact, this latter is characterized by four peaks situated at 881.5, 885.7, 899.6 and 904.0 eV (Fig. 4b) [18]. It has been demonstrated [18] that Ce(III)/Ce(IV) ratio variation, observed on the surface of the analysed sample strongly affects the absolute binding energy positions of the Ce3d XPS spectra. Notice that a shift was observed on our samples when the vanadium content changed. On the other side, some authors [33] have elaborated different relations to quantify the Ce(III) and Ce(IV) concentration in a given sample. The results obtained from the analysis of a pure CeO_2 powder show that the satellite peak (~916.5 eV) contribution represents 12.75% of the total Ce3d intensity. This percentage decreased to 10.16 and 9.05%

for 1.67V10Ce and 5.06V10Ce samples respectively. These diminutions can be interpreted by the partial reduction of Ce^{4+} ions of the CeO_2 surface into Ce^{3+} species. The vanadyl groups of the oxalate added on the ceria surface is responsible of that reduction to form the oxalate of vanadium(V)–cerium(III) complex as it was mentioned above.
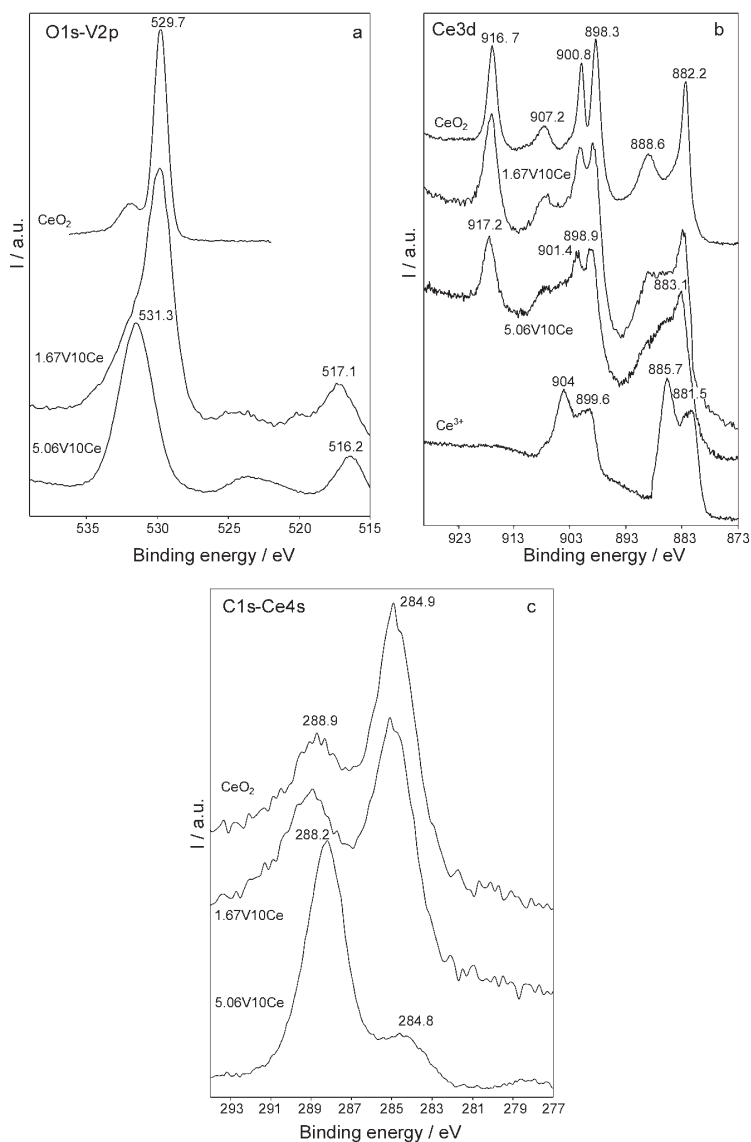
Fig. 4 XPS spectra of 1.08V10Ce and 5.06V10Ce samples: (a) V2p and O1s XPS spectra; (b) Ce3d XPS spectra and (c) C1s and Ce4s XPS spectra

The XPS peak obtained at ~288 eV (Fig. 4c) can be characteristic of C1s and Ce4s [35–36] binding energies. Indeed, a similar peak was observed in the case of sodium oxalate [36] and was assigned to carboxyl group of this complex. In parallel, the same peak with the same binding energy was obtained for CeO_2 solid [37–39] and was interpreted as the photoelectron energy of Ce4s. Whereas, it is well-known that the XPS of cerium(IV) is also characterized by the presence of six peaks corresponding to Ce3d. The relative intensity ratio $I_{Ce4s}/I_{Ce3d}=9.12\cdot10^{-3}$ of the XPS cerium spectrum remains unchanged. Since, it was demonstrated for 1.67V10Ce sample that this ratio ($11.7\cdot10^{-3}$) is larger than that obtained for pure ceria, this indicates that the peak observed in our case is the superposition of two peaks: the first corresponding to Ce4s of CeO_2 phase and the second to C1s of oxalate group. The intensity of the ~288 eV peak significantly increased for 5.06V10Ce sample, this is mainly due to the carbon of oxalates and not to cerium. Indeed, the surface analysis of this latter sample shows that the atomic ratio O/C=2.28 measured is approximately in the same order of that corresponding to the oxalate group (O/C=2). The slight difference in the atomic ratios obtained can be explained by the participation of the O1s photo peak relative to cerium and vanadium oxides present on the surface with that corresponding to oxalate group.

More information can also be obtained by comparison of O1s XPS spectra (Fig. 4a). Indeed, it is well-known that XPS peaks characterized by binding energies situated in the range of 529–533 eV are due to oxygen species (O1s) present in different matrices [36–40]. The low-binding energy component in the range of 529.3±0.3 eV is ascribable to oxygen of oxides, whereas high-binding energy components (531.7±0.3 eV) are due either to hydroxide species or to carboxyl groups. On the 1.67V10Ce sample, the O1s binding energy measured (529.8 eV) is smaller than that obtained on 5.06V10Ce (531.3 eV) (Fig. 4c). For 5.06V10Ce sample, the binding energy is larger than that corresponding to oxygen of the pure ceria (529.7 eV). This increase can be related to the oxygen of oxalate which became mainly dominant with the increase of the vanadyl precursor content and consequently responsible of the binding energy shift toward the high values.

Conclusions

When CeO_2 phase is impregnated by a vanadyl oxalate solution, three types of oxalate were evidenced on the untreated solids: i) vanadium(V) oxalate attached to cerium(III) of the ceria phase seems be formed and remains thermally stable till 170–190°C, ii) vanadyl oxalate remaining in excess on ceria up to 260–300°C and iii) cerium oxalate which thermally decomposes at 310°C.

* * *

References

1 H. C. Yao and Y. F. Yu Yao, J. Catal., 86 (1984) 254.
2 A. Trovarelli, Catal. Rev.-Sci. and Eng., 38 (1996) 439.
3 S. Tagliaferri, R. A. Köppel and A. Baiker, Appl. Catal. B, 15 (1998) 159.
4 J. Kašpar, P. Fornasiero and M. Graziani, Catal. Today, 50 (1999) 285.
5 R. H. Nibbelke, A. J. L. Nievergeld, J. H. B. J. Hoebink and G. B. Marin, Appl. Catal. B, 19 (1998) 245.
6 J. R. González-Velasco, M. A. Gutiérrez-Ortiz, J. L. Marc, J. A. Botas, M. P. Gonzalez-Marcos and G. Blanchard, Appl. Catal. B, 22 (1999) 167.
7 B. Grzybowska-Swierkosz, Appl. Catal., 157 (1997) 263.
8 A. F. Ahlström-Odenbrand, Appl. Catal., 60 (1990) 157.
9 L. Lietti and P. Forzatti, J. Catal., 147 (1994) 241.
10 A. J. van Hegstum, J. G. van Ommen, H. Bosch and P. J. Gellings, Appl. Catal., 8 (1983) 369.
11 J. Kijenski, A. Baiker, M. Gliski, P. Dollenmeier and A. Wokaun, J. Catal., 101 (1986) 1.
12 V. K. Sharma, A. Wokaun and A. Baiker, J. Phys. Chem., 90 (1986) 2715.
13 P. Roman, C. Guzman-Miralles, A. Luque, J. I. Beitia, J. Cano, F. Lioret, M. Julve and S. Alvarez, Inorg. Chem., 35 (1996) 3741.
14 F. Bérézovsky, A. A. Hajem, S. Triki, J. Sala Pala and P. Molinnié, Inorg. Chim. Acta, 284 (1999) 8.
15 S. Triki, F. Bérézovsky, J. Sala Pala, E. Coronado, C. J. Gomez-Garcia, J. M. Clemente, A. Riou and P. Molinié, Inorg. Chem., 39 (2000) 3771.
16 A. M. Donia, N. R. E. Radwan and A. A. Atia, J. Therm. Anal. Cal., 61 (2000) 249.
17 R. Cousin, S. Capelle, E. Abi-Aad, D. Courcot and A. Aboukaïs, Chem. Mat., in press.
18 E. Abi-Aad, R. Bechara, J. Grimblot and A. Aboukaïs, Chem. Mater., 5 (1993) 793.
19 A. Tsoga, A. Naoumidis, W. Jungen and D. Stover, J. Europ. Ceram. Soc., 19 (1999) 907.
20 G. A. M. Hussein and H. M. Ismail, Colloids Surfaces A: Physicochem. Eng. Aspects, 95 (1995) 53.
21 M. V. John and M. A. Yttiachen, Bull. Mater. Sc., 21 (1998) 387.
22 A. Aboukaïs, A. Bennani, C. F Aissi, G. Wrobel and M. Guelton, J. Chem. Soc., Faraday Trans., 88 (1992) 1321.
23 E. A. Zhilinskaya, F. Delmaire, A. Rives, M. Rigole, R. Hubaut and A. Aboukaďs, (Russ.) J. Phys. Chem., 73 (1999) 1960.
24 I. Eguchi, T. Furusawa, T. Miura and T. Kishi, Solid State Ionics, 68 (1994) 159.
25 E. Buglyo, E. Kiss, I. Fabian, T. Kiss, D. Sanna, E. Garriba and G. Micera, Inorganica Chimica Acta, 306 (2000) 174.
26 V. F. Anufrienko, A. A. Altynnikov and N. N. Chumachenko, React. Kinet. Catal. Lett., 48 (1992) 589.
27 L. Cornaglia and E. Lombardo, Appl. Catal. A. : General, 23 (1995) 125.
28 V. Bukhtiyarov, P. Albers, M. Baerns, B. Bal'zhinimaev, G. Bond, A. Brueckner, L. Gengembre, M. J. Genet, M. Delamar, M. Guelton, J. Kiwi, J. Ph Nogier, I. P. Prosvirin, A. O. Taylor and I. York, Catal. Today, 56 (2000) 403.
29 Y. Chen, K. Xie and Z. X. Liu, Appl. Surf. Science, 133 (1998) 221.
30 M. Matsko, I. Prosvirin, T. Mikenas, V. Zakharov, E. Paukshits, V. Bukhtiyarov and I. Danilova, J. Molec. Catal. A: Chemical, 158 (2000) 443.
31 Y-J. Kim, Y-I. Kim and S-N. Choi, Polyhedron, 19 (2000) 2155.

32 A. Kotani, T. Jo and T. C. Parlebas, Adv. Phys., 37 (1988) 37.

33 J. Shyu, K. Otto, W. Wattkins, G. Graham, R. Belitz and H. Gandhi, J. Catal., 114 (1988) 23.

34 K. S. Sim, L. Hilaire, F. Le Normand, R. Touroude, V. Paul-Boncour and
A. Percheron-Guegan, J. Chem. Soc. Faraday Trans., 87 (1991) 1453.

35 C. Padeste, N. Cant and D. Trimm, Catal. Lett., 18 (1993) 305.

36 D. Bonerjee and H. W. Nesbitt, Geochim. Cosmochim. Acta, 19 (1999) 3025.

37 J. Z. Shyu, K. Otto, W. L. H. Watkins, G. W. Graham, R. K. Belitz and H. S. Gandhi, J. Catal.,
114 (1988) 23.

38 A. Kotani, T. Jo and J. C. Parlebas, Adv. Phys., 115 (1988) 16.

39 R. Cousin, M. Dourdin, E. Abi-Aad, D. Courcot, S. Capelle, M. Guelton and A. Aboukaïs,
J. Chem. Soc., Faraday Trans., 93 (1997) 3863.

40 W. Fitzgerald, J. Foley, Mc Sweene, N. Ray, D. Sheahan, S. Tyaga, B. Hathaway and
P. O. Brien, J. Chem. Soc. Dalton Trans., (1982) 1117.